

TRIPLE BARS AND COMPLEX CENTRAL STRUCTURES IN DISK GALAXIES

PETER ERWIN AND LINDA S. SPARKE

University of Wisconsin-Madison

Accepted by The Astrophysical Journal Letters

ABSTRACT

We present an analysis of ground-based and HST images of three early-type barred galaxies. The first, NGC 2681, may be the clearest example yet of a galaxy with three concentric bars. The two other galaxies were previously suggested as triple-barred. Our analysis shows that while NGC 3945 is probably double-barred, NGC 4371 has only one bar; but both have intriguing central structures. NGC 3945 has a large, extremely bright disk inside its primary bar, with patchy dust lanes, a faint nuclear ring or pseudo-ring within the disk, and an apparent secondary bar crossing the ring. NGC 4371 has a bright nuclear ring only marginally bluer than the surrounding bulge and bar. There is no evidence for significant dust or star formation in either of these nuclear rings. The presence of stellar nuclear rings suggests that the centers of these galaxies are dynamically cool and disklike.

Subject headings: galaxies: structure — galaxies: active — galaxies: individual (NGC 2681, NGC 3945, NGC 4371)

1. INTRODUCTION

Many double-barred galaxies — those with a smaller, concentric bar inside the main bar — have been found in recent years; see Friedli (1996) for a review. Erwin & Sparke (1999) find secondary bars in at least 20% of their sample of barred S0–Sa field galaxies. Wozniak et al. (1995, hereafter W95) and Friedli et al. (1996) noted three galaxies that appeared to have *three* concentric bar-like structures. Bars-within-bars have been advocated as a way to bring gas into the nucleus of galaxies (e.g., Shlosman, Frank, & Begelman 1989). Pfenniger & Norman (1990) studied dissipative motion in a system with the inner bar rotating faster than the outer one, while Maciejewski & Sparke (1997) showed how these might be modeled as self-consistent dynamical systems, with particle orbits reproducing the shape of the potential. Here, we present optical images from our survey with the 3.5m WIYN telescope and archival optical and near-IR images from the Hubble Space Telescope (HST) for two of W95’s triple-bar candidates, NGC 3945 and NGC 4371, and a third galaxy, NGC 2681.¹

2. OBSERVATIONS AND ANALYSIS

Images were analyzed using the IRAF ellipse package, which fits ellipses to isophotes (Jedrzejewski 1987). We identified bars by visual inspection of the images and by looking for peaks in isophote ellipticity that were accompanied by stationary values of the position angle, as described by W95. We also created unsharp masks, to look for subtle, small-scale brightness variations and structures not otherwise readily apparent. Table 1 lists the main features we found.

NGC 2681, Figure 1: This galaxy is close to face-on; outer disk isophotes have ellipticity < 0.07 . Thus, the three barlike structures cannot be projection effects. The outermost bar is relatively large, though not outside the

range for early-type galaxies found by Martin (1995). Although this structure is relatively faint, the PA is nearly stationary at $\approx 30^\circ$ for $a \approx 45\text{--}60''$ (1c). At these radii, the isophotes have the squared-off ends (1a, d) characteristic of bars in early-type galaxies (Athanasoula et al. 1990). Consequently, we feel reasonably confident that this *is* a bar. The NICMOS image confirms the existence of a third bar — tentatively identified by W95 and Friedli et al. (1996) as the galaxy’s secondary bar.

NGC 3945, Figure 2: Interpretation of structures in this galaxy depends strongly on what inclination is assumed. W95 suggested that $i = 26^\circ$, and that the galaxy is triply barred. For two reasons, we feel that an inclination of $\sim 50^\circ$ is more likely, and that their secondary bar is probably an axisymmetric structure. The primary bar ($a \approx 40''$) is surrounded by outer and inner rings (2d, g); both appear perpendicular to the bar. Inner rings are almost always elongated *parallel* to the bar (Buta 1986, 1995). If the inner ring is intrinsically circular, then $i \approx 35^\circ$; $i \approx 50^\circ$ for a typical axis ratio ($b/a = 0.78$, Buta 1995). The kinematics also imply a high inclination: Kormendy (1982) measured stellar speeds of $\approx 250 \text{ km s}^{-1}$ in the lens region, while the H I profile has a half-width of 340 km s^{-1} (Wardle & Knapp 1986). If $i = 26^\circ$, then the circular velocity reaches an astonishing $V \sim 780 \text{ km s}^{-1}$, higher even than in the fastest-rotating disk galaxy known, UGC 12591 (Giovanelli et al. 1986, $V \approx 500 \text{ km s}^{-1}$). For $i = 50^\circ$, we would have $V \sim 440 \text{ km s}^{-1}$.

Our fits (2c) show *seven* ellipticity peaks — including the outer and inner rings — all but two of which are within position angles $155\text{--}160^\circ$. At least some of the latter structures are probably near-axisymmetric, viewed at an inclination of $\sim 50^\circ$. Kormendy (1993) has pointed out that the fast rotation and relatively low velocity dispersion in the “bulge” region ($a < 20''$) of this galaxy suggest a disk rather than a bulge. The structure W95 called a “sec-

¹The WIYN Observatory is a joint facility of the University of Wisconsin-Madison, Indiana University, Yale University, and the National Optical Astronomy Observatories. Observations with the NASA/ESA Hubble Space Telescope obtained at the Space Telescope Science Institute, operated by the Association of Universities for Research in Astronomy, Inc., under NASA contract NAS5-26555.

ondary bar” (the ellipticity peak at $a \approx 10''$) is thus probably intrinsically round and flat — an inner disk. Assuming that it is vertically thin, the measured ellipticity of 0.36 deprojects to a circle if $i = 50^\circ$.

Unsharp masking (2e, f) shows a nuclear ring or tight spiral with $a \approx 6.5''$. At $a \approx 2.5\text{--}3''$, the WFPC2 images show a possible foreshortened secondary bar crossing the ring. The weak innermost ellipticity peak at $a < 2''$, W95’s “tertiary bar”, shares the common system alignment; the galaxy center is probably mildly oblate rather than barred. The $V-I$ color map (2h) shows complex dust structures within the nuclear ring.

NGC 4371, Figure 3: W95 identified a “secondary bar” at $a \approx 10''$, aligned to within a few degrees of the outer disk; they noted that it could be a projection effect, due to the galaxy’s high inclination. Our unsharp mask (3e) shows that this feature is a smooth nuclear ring, rather than a bar, with no signs of dust or ongoing star formation. Kormendy (1982, 1993) noted disk-like dynamics in the bulge region; the ring may be partially responsible. The stellar ring is marginally bluer than the surrounding bulge, or may be surrounded by a weak dust ring; cf. the red ring noted by W95. The very center of the galaxy shows twisted, spiral isophotes (3f), possibly due to a dusty nuclear disk.

3. DISCUSSION

At HST resolution, NGC 2681 proves to have three distinct bars; NGC 3945 has two. The relative orientation of the nested bars appears random, as expected if the components rotate independently, and in line with the findings

of Friedli (1996). Both galaxies with multiple bars have LINER nuclei, while NGC 4371 does not; this is weak evidence in favor of Shlosman et al.’s (1989) thesis that inner bars can enhance nuclear fuelling (but see Mulchaey & Regan 1997).

“Bars” closely aligned with outer-disk isophotes must be treated with suspicion: they may be flat, axisymmetric structures in projection. Combining unsharp masking with ellipse fits, we find a nuclear ring in NGC 4371 and a bright disk-plus-ring in the inner regions of NGC 3945. Neither ring shows signs of current star formation; they may be part of a previously overlooked population of older, stellar nuclear rings in early-type galaxies. A dynamically “hot” stellar system like a bulge, where the velocity dispersion σ is of the same magnitude as the rotation speed V , does not form bars or rings; these are characteristic of “cool” disks, where V is at least a few times larger than σ . So the wealth of features revealed in these high-resolution images reinforces Kormendy’s (1993) suggestion: the bright inner regions of many galaxies may be dominated by dynamically cool disks rather than dynamically hot bulges.

We would like to thank Jay Gallagher for useful comments throughout this work, and the referee, Daniel Friedli, for helpful criticism. This research was supported by NSF grant AST-9320403, and NASA grants NAGW-2796 and AR-0798.01-96A from the Space Telescope Science Institute, operated by the Association of Universities for Research in Astronomy, Inc., under NASA contract NAS5-26555.

REFERENCES

- Athanassoula, E., Morin, S., Wozniak, H., Puy, D., Pierce, M. J., Lombard, J., & Bosma, A. 1990, *MNRAS*, 245, 130
 Buta, R. 1986, *ApJS*, 61, 609
 Buta, R. 1995, *ApJS*, 96, 39
 de Vaucouleurs, G., de Vaucouleurs, A., Corwin, H. G., Buta, R. J., Paturel, G., & Fouqué, P. 1991, *Third Reference Catalogue of Bright Galaxies* (New York: Springer-Verlag) (RC3)
 Erwin, P., & Sparke, L. S. 1999, in *Galaxy Dynamics*, ed. D. R. Merritt, M. Valluri, & J. A. Sellwood, in press
 Friedli, D., Wozniak, H., Rieke, M., Martinet, L., & Bratschi, P. 1996, *A&AS*, 118, 461
 Friedli, D. 1996, in *IAU Colloquium 157: Barred Galaxies*, ed. R. Buta, B. G. Elmegreen, & D. A. Crocker (San Francisco: ASP), 378
 Giovanelli, R., Haynes, M. P., Rubin, V. C., & Ford, W. K. 1986, *ApJ*, 301, L7
 Ho, L. C., Filippenko, A. V., & Sargent, W. L. W. 1997, *ApJS*, 112, 391
 Jedrzejewski, R. I. 1987, *MNRAS*, 226, 747
 Kormendy, J., 1982, *ApJ*, 257, 75
 Kormendy, J., 1993, in *Galactic Bulges*, IAU Symposium 153, ed. H. Dejonghe & H. J. Habing (Dordrecht: Kluwer), 209
 Maciejewski, W., & Sparke, L. S. 1997, *ApJ*, 484, L117
 Martin, P. 1995, *AJ*, 109, 2428
 Mulchaey, J. S., & Regan, M. W. 1997, *ApJ*, 482, L135
 Pfenniger, D., & Norman, C. 1990, *ApJ*, 363, 391
 Shlosman, I., Frank, J., & Begelman, M. C. 1989, *Nature*, 338, 45
 Wardle, M., & Knapp, G., 1986, *AJ*, 91, 23
 Wozniak, H., Friedli, D., Martinet, L., Martin, P., & Bratschi, P. 1995, *A&A*, 111, 115 (W95)

TABLE 1

Galaxy	Type (RC3)	Nucleus	Features				
NGC 2681	(R')SAB(rs)0/a	LINER	Outer Disk $r_{25} = 110''$ PA = 130°	Bar 1 $a = 50\text{--}60''$ 30°	Bar 2 $15\text{--}20''$ 75°	Bar 3 $1.8\text{--}4.0''$ 20°	
NGC 3945	SB(rs)0 ⁺	LINER	Outer Ring $a = 150''$ PA = 160°	Bar 1 $30\text{--}40''$ 75°	Disk $10''$ 158°	Nuclear Ring $6.5''$ 158°	Bar 2 $2.5\text{--}3.0''$ 115°
NGC 4371	SB(r)0 ⁺	No activity	Outer Disk $r_{25} = 120''$ PA = 92°	Bar 1 $a = 34\text{--}40''$ 158°		Nuclear Ring $10.5''$ 92°	

NOTE.—Nuclear classifications are from Ho, Filippenko, & Sargent 1997, radii r_{25} are from de Vaucouleurs et al. 1991 (RC3). Position angle PA is measured from ellipse fits, where ellipticity is maximal (ϵ_{max}). Semi-major axis a is that at ϵ_{max} for disks and rings. Lower limit to bar length is at ϵ_{max} ; upper limit is the point outside outside ϵ_{max} where PA has changed by 10° . Features with $a < 30''$ are measured using fits to HST images (see Figures 1c, 2c, 3c); larger features are measured using WIYN R-band images. No deprojections were attempted.

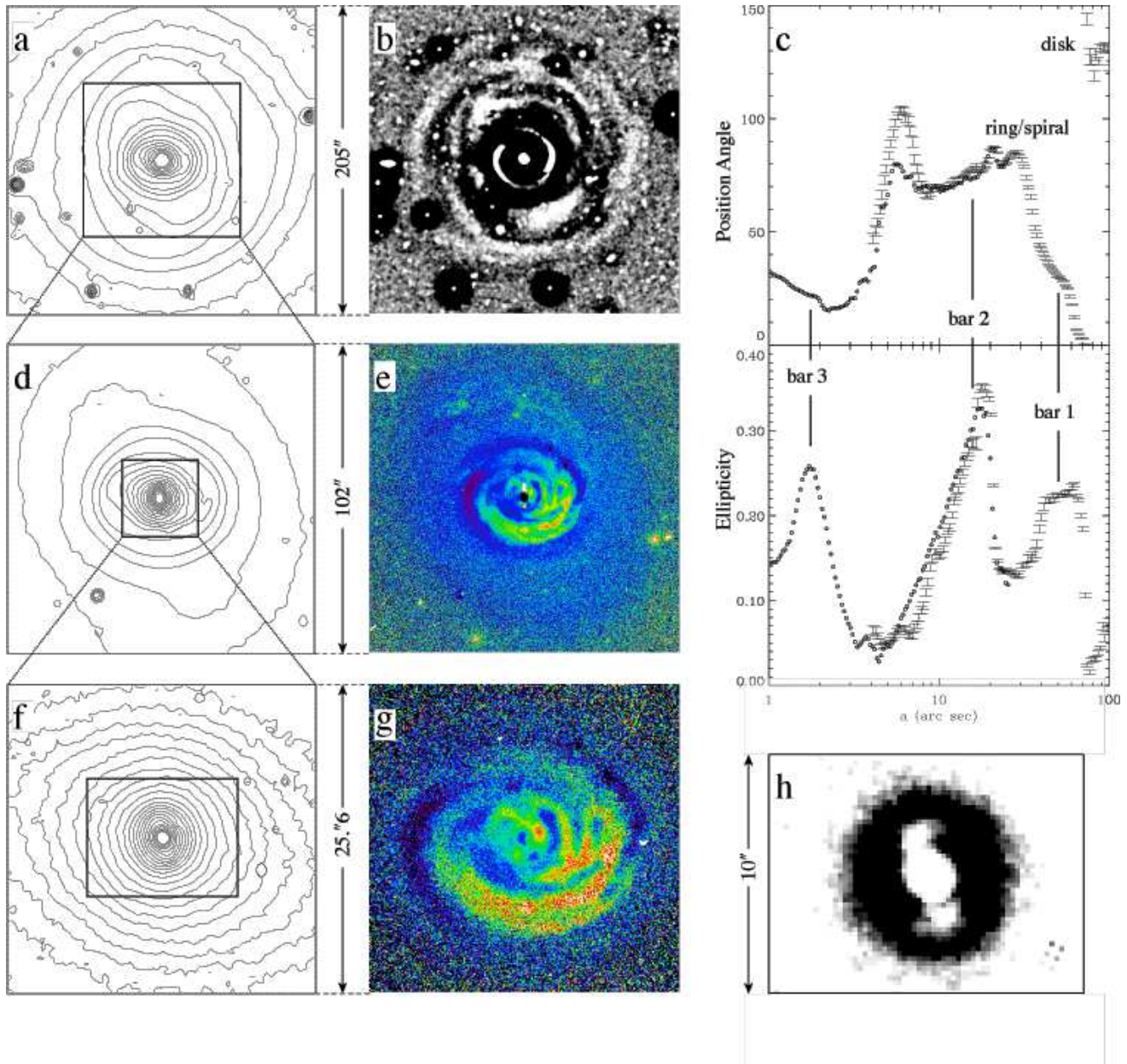


FIG. 1.— North is up and east is to the left in all images; no deprojection has been attempted. NGC 2681: **a** WIYN R-band image: contour plot of the square root of logarithmic brightness, showing outer disk, primary and secondary bars. **b** Unsharp mask, showing inner and outer rings; dark circles are due to foreground stars. **c** Isophotal ellipse fits to WIYN R-band (error bars) and NICMOS3 F160W (circles) images. **d** R-band image, logarithmic brightness contours. **e** Median-smoothed $B-R$ color map. The nucleus is affected by saturation. **f** NICMOS3 F160W image, showing tertiary bar. **g** WIYN $B-R$ colormap (no saturation, unsmoothed) for the same region; the blue center is probably the LINER nucleus. **h** Unsharp mask of boxed region of panel f, showing possible spiral arms outside the tertiary bar.

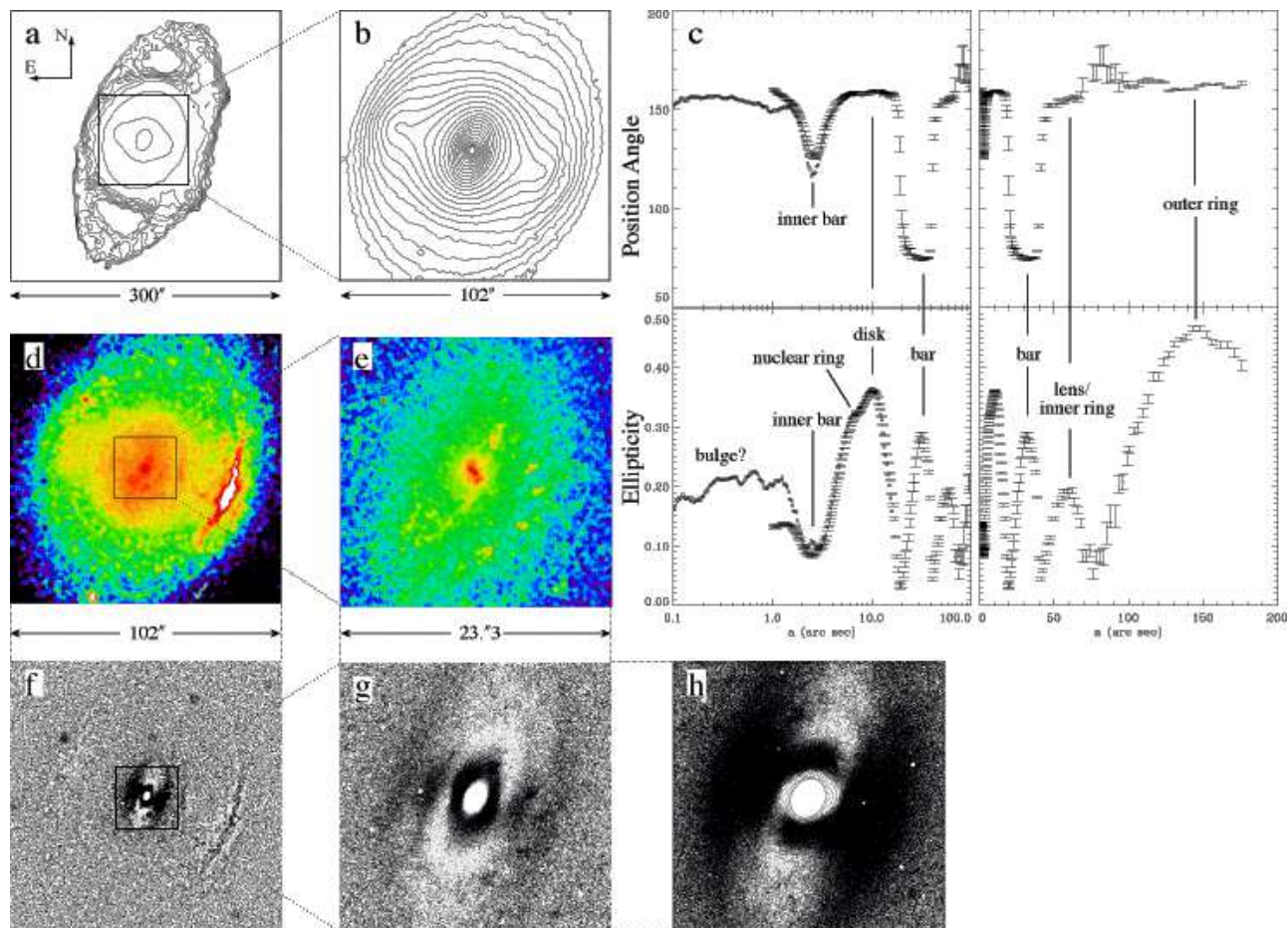


FIG. 2.— NGC 3945: **a** and **b** WIYN R-band images, logarithmically scaled. **c** Isophotal ellipse fits to WIYN R-band (error bars) and WFPC2 F814W (circles) images: left, on a logarithmic scale; right, on a linear scale. **d** Median-smoothed WIYN $B-R$ color map shows dust in the inner ring and inner disk. **e** WFPC2 $V-I$ ($F555W-F814W$) color map, showing dust clumps west of the nucleus and inside the nuclear ring; the ring itself is not apparent. **f** Unsharp mask of WIYN B-band image on the same scale as **b**, showing the dusty inner ring on both sides of the main bar. **g** Unsharp mask of F814W image, showing the nuclear ring and short dust lanes in the western disk. **h** as for **g** but with a higher level of smoothing used for the mask, to show larger scale features better. Contours show the partly spiral nature of the inner ring, crossed by an apparent inner bar.

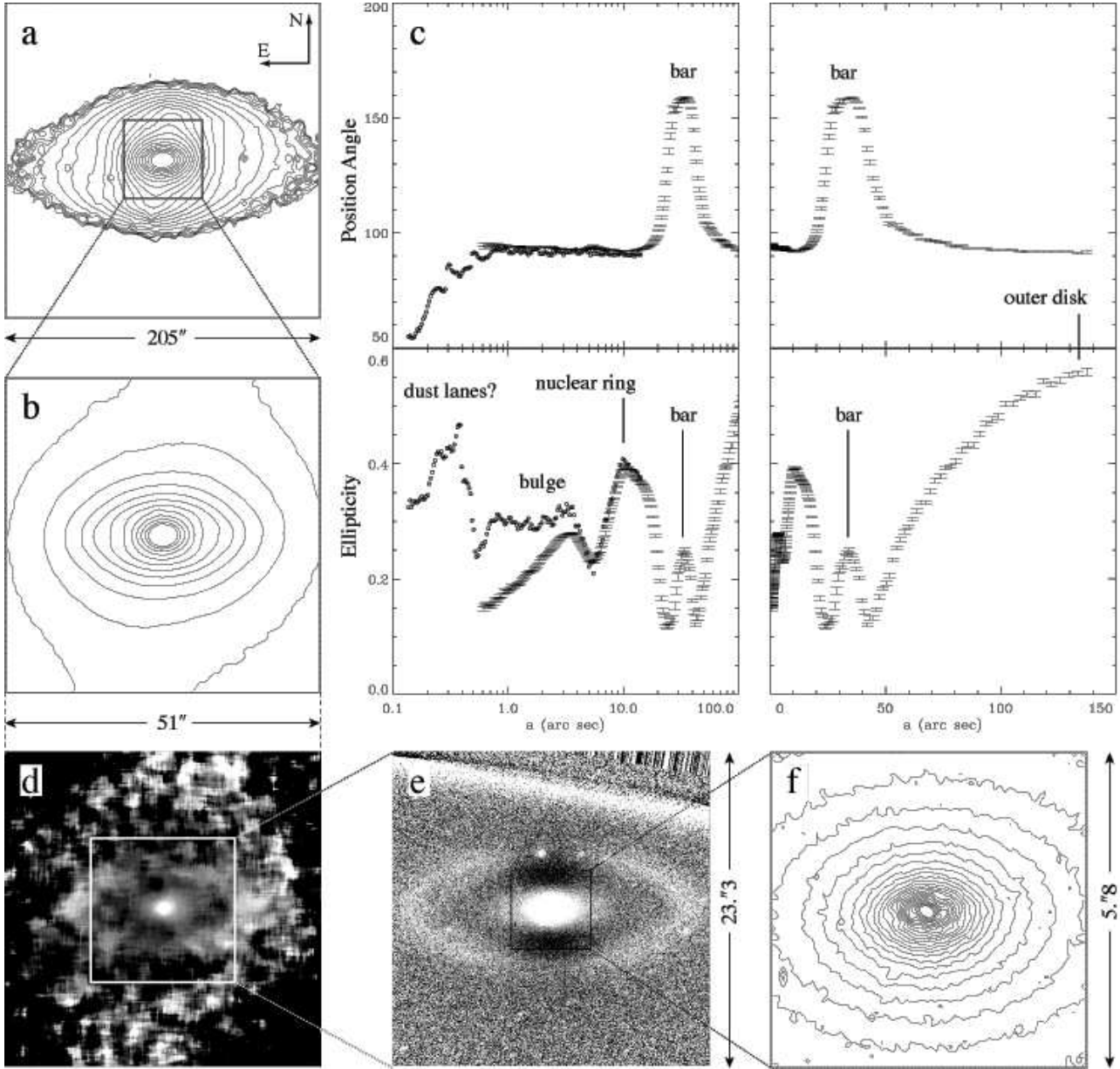


FIG. 3.— NGC 4371: **a** WIYN R-band image: contour levels are square root of logarithmic brightness. **b** WIYN R-band image, logarithmic contours; note boxy isophotes inside the ring ($a < 10''$). **c** Ellipse fits to isophotes for WIYN R-band (error bars) and WFPC2 F555W (circles) images. **d** Median-smoothed $B-R$ color map from WIYN images; lighter areas are redder. The apparent ring at $a \approx 15''$ is at most 0.05 magnitudes redder in $B-R$ than the nuclear ring. **e** Unsharp mask of the F555W image, showing the nuclear ring, with apparent ellipticity ≈ 0.6 and $a \approx 10''$. The bright line crossing at the top is the edge of the PC2 chip. **f** Twisted isophotes in the center of the WFPC2 image, perhaps due to dust.